

# Dimetalocene Carbonyls of the Third-Row Transition Metals: The Quest for High-Order Metal–Metal Multiple Bonds<sup>†</sup>

Bing Xu,<sup>‡</sup> Qian-Shu Li,<sup>\*,‡,§</sup> Yaoming Xie,<sup>||</sup> R. Bruce King,<sup>\*,§,||</sup> and Henry F. Schaefer III<sup>||</sup>

*Institute of Chemical Physics, Beijing Institute of Technology, Beijing 100081, China, Center for Computational Quantum Chemistry, South China Normal University, Guangzhou, 510631 China, and Department of Chemistry and Center for Computational Chemistry, University of Georgia, Athens, Georgia 30602*

*Received: April 15, 2009; Revised Manuscript Received: June 29, 2009*

Theoretical studies of the third-row transition-metal derivatives  $\text{Cp}_2\text{M}_2(\text{CO})$  ( $\text{Cp} = \eta^5\text{-C}_5\text{H}_5$ ;  $\text{M} = \text{Os}, \text{Re}, \text{W}, \text{Ta}$ ) indicate that the lowest-energy structures have lower spin states and similar or higher metal–metal bond multiplicities than the corresponding first-row transition-metal derivatives. Therefore,  $\text{Cp}_2\text{Os}_2(\text{CO})$  is predicted to be a singlet with an Os–Os formal quadruple bond, whereas  $\text{Cp}_2\text{Fe}_2(\text{CO})$  is a triplet. Similarly,  $\text{Cp}_2\text{Re}_2(\text{CO})$  is predicted to be a singlet with a very short rhenium–rhenium distance, which is consistent with the formal quintuple bond required to give both rhenium–rhenium atoms the favored 18-electron configuration. This contrasts with the manganese analogue  $\text{Cp}_2\text{Mn}_2(\text{CO})$  for which the lowest-energy structure is a septet with a formal Mn–Mn single bond. The tungsten derivative  $\text{Cp}_2\text{W}_2(\text{CO})$  is predicted to be triplet with a four-electron donor bridging carbonyl group. This contrasts with  $\text{Cp}_2\text{Cr}_2(\text{CO})$  predicted to be a septet ( $S = 3$ ) with a two-electron donor carbonyl group. For  $\text{Cp}_2\text{Ta}_2(\text{CO})$ , the lowest-energy structure is predicted to be a triplet with a formal Ta≡Ta triple bond and a four-electron donor carbonyl group. However,  $\text{Cp}_2\text{V}_2(\text{CO})$  is predicted to be a quintet with a formal V=V double bond. In addition to these  $\text{Cp}_2\text{M}_2(\text{CO})$  structures with one Cp ring bonded to each metal atom, higher-energy  $\text{Cp}_2\text{M}-\text{MCO}$  structures are found with both Cp rings bonded to the same metal atom. The lowest-energy  $\text{Cp}_2\text{M}-\text{MCO}$  structures are triplets ( $\text{M} = \text{Os}, \text{W}$ ) or quintets ( $\text{M} = \text{Re}$ ) with agostic hydrogen atoms for  $\text{M} = \text{Os}$  and  $\text{Re}$ . In these structures, the spin density is concentrated on the metal atom of the MCO group. These results suggest that lower spin states clearly become more viable for highly unsaturated metal complexes upon descending the periodic table.

## 1. Introduction

The chemistry of metal–metal multiple bonding<sup>1,2</sup> dates back to the pioneering work of Cotton and Harris<sup>3</sup> in 1965 on the rhenium–rhenium quadruple bond in the binuclear metal halide complex  $\text{Re}_2\text{Cl}_8^{2-}$  (Figure 1). This was not only the first example of a metal–metal quadruple bond but also the first example of a quadruple bond of any type. Such a quadruple bond can be considered to consist of a  $\sigma$  component, two orthogonal  $\pi$  components, and one  $\delta$  component (Figure 1). The  $\delta$  component of such a quadruple bond (green in Figure 1) is relatively weak compared with (at least) the  $\pi$  components (blue in Figure 1) because of the much poorer overlap of the relevant metal  $d$  orbitals.

In principle, this bonding model for the metal–metal quadruple bond (Figure 1) can be extended to a metal–metal quintuple bond by using a second metal  $d$  orbital of  $\delta$  symmetry rotated 45° about the metal–metal axis so that the two  $\delta$  components of such a metal–metal quintuple bond do not overlap with each other. An isolable compound with such a metal–metal quintuple bond was realized only in 2005 by Power et al.,<sup>4</sup> who synthesized a binuclear chromium(I) aryl of the type  $\text{RCrCrR}$  with an extremely short metal–metal distance, suggesting such a quintuple bond. Therefore, the discovery of

the first compound with a metal–metal quintuple bond was achieved 40 years after the discovery of the first compound with a metal–metal quadruple bond. Furthermore, this discovery has prompted a number of recent theoretical studies on metal–metal quintuple bonding.<sup>5–8</sup>

The first example of a stable metal carbonyl derivative containing a metal–metal multiple bond dates back to 1967 when King and Bisnette<sup>9</sup> synthesized  $(\eta^5\text{-Me}_5\text{C}_5)_2\text{Mo}_2(\text{CO})_4$  (Figure 2). Their suggestion of an Mo≡Mo triple bond in this structure on the basis of the 18-electron rule<sup>10,11</sup> was later supported by an X-ray structural determination indicating an unusually short metal–metal distance consistent with a triple bond. Therefore, the metal–metal distance in  $(\eta^5\text{-Me}_5\text{C}_5)_2\text{Mo}_2(\text{CO})_4$  was found to be 2.49 Å as compared with 3.24 Å for  $(\eta^5\text{-C}_5\text{H}_5)_2\text{Mo}_2(\text{CO})_6$ , which clearly has a metal–metal single bond.<sup>12</sup> Shortly thereafter, the analogous chromium compounds  $(\eta^5\text{-R}_5\text{C}_5)_2\text{Cr}_2(\text{CO})_4$  ( $\text{R} = \text{H},^{13} \text{Me}^{14,15}$ ) were also prepared and likewise found to have relatively short Cr≡Cr distances around 2.24 Å, suggesting triple bonds. Subsequent work led to the discovery of the related binuclear cyclopentadienylmetal carbonyls  $\text{Cp}_2\text{V}_2(\text{CO})_5$ <sup>16,17</sup> and  $\text{Cp}_2\text{M}'_2(\text{CO})_3$  ( $\text{M}' = \text{Mn},^{18} \text{Re}^{19}$ ) (Figure 2). The structures of all of these binuclear cyclopentadienylmetal carbonyls are shown by X-ray diffraction to have the short metal–metal distances expected for the formal triple bonds required to give the metal atoms the favored 18 electrons. No stable binuclear cyclopentadienylmetal carbonyls with formal metal–metal bond orders of four and five have been synthesized yet.

<sup>†</sup> Part of the “Russell M. Pitzer Festschrift”.

\* Corresponding authors. E-mail: rbking@chem.uga.edu (R.B.K.); qqli@sncu.edu.cn (Q.-S.L.).

<sup>‡</sup> Beijing Institute of Technology.

<sup>§</sup> South China Normal University.

<sup>||</sup> University of Georgia.

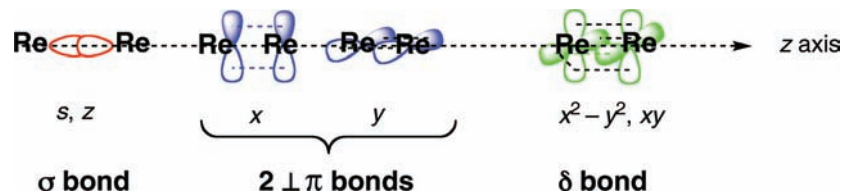


**Figure 1.** Components of the Re–Re quadruple bond in  $\text{Re}_2\text{Cl}_8^{2-}$  and related compounds. The  $\sigma$ ,  $\pi$ , and  $\delta$  components of the quadruple bond are in red, blue, and green, respectively.

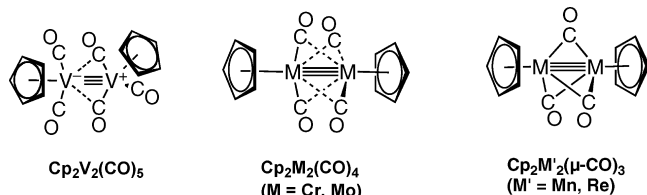


**Figure 2.** Stable binuclear cyclopentadienylmetal carbonyls with formal metal–metal triple bonds that have been structurally characterized by X-ray diffraction.

This article discusses a search for high-order metal–metal bonds in binuclear cyclopentadienylmetal carbonyls using density functional theory (DFT). Derivatives of the type  $\text{Cp}_2\text{M}(\text{CO})$  ( $\text{Cp} = \eta^5\text{-C}_5\text{H}_5$ ), that is, “dimetalocene carbonyls,” were selected for this research to have the maximum number of metal orbitals available for high-order multiple bonds after accommodating the bonds to the cyclopentadienyl ring and carbonyl group. The third-row transition metals Ta, W, Re, and Os were chosen for this study to maximize the stability of singlet spin states relative to higher spin states so that the maximum number of electrons are paired for components of a metal–metal multiple bond, thereby increasing its formal bond order. The results are compared with a previous study<sup>20</sup> of  $\text{Cp}_2\text{M}(\text{CO})$  derivatives containing the first-row transition metals Ti, V, Cr, and Mn. In this work, short metal–metal distances are considered to be diagnostic of metal–metal bonds of high formal order. Previous experience with other metal–metal multiply bonded carbonyl derivatives has shown that a detailed molecular orbital analysis of such metal–metal bonds is complicated by competing interactions of metal orbitals with ligand orbitals, the low symmetry of the structures, and the weakness of the  $\delta$  components of metal–metal bonds of order four and higher.

## 2. Theoretical Methods

We considered electron correlation effects by employing DFT, which has evolved as a practical and effective computational tool, especially for organometallic compounds.<sup>21–35</sup> In this work, two DFT methods BP86 and MPW1PW91 were used. The BP86 method is a pure DFT method that combines Becke’s 1988 exchange functional with Perdew’s 1986 correlation functional.<sup>36,37</sup> The MPW1PW91 method<sup>38</sup> is a so-called second-generation<sup>39</sup> functional that combines the modified Perdew–Wang exchange functional with Perdew–Wang’s 1991 correlation functional.<sup>40</sup> The MPW1PW91 method has been found to be more suitable for geometry optimization of the second- and third-row transition-metal systems,<sup>41,42</sup> whereas the BP86 method usually provides better vibrational frequencies with DZP basis sets.

For the third-row transition metals, the large numbers of electrons may increase the computational efforts exponentially. To reduce the cost, effective core potential (ECP) relativistic basis sets are employed. The SDD (Stuttgart–Dresden ECP plus DZ)<sup>43</sup> ECP basis set was used for the Os, Re, W, and Ta atoms. For the C and O atoms, the double- $\zeta$  plus polarization (DZP) basis sets were used. The latter are the Huzinaga–Dunning

contracted double- $\zeta$  sets<sup>44,45</sup> plus a set of spherical harmonic d-polarization functions with orbital exponents  $\alpha_d(\text{C}) = 0.75$  and  $\alpha_d(\text{O}) = 0.85$ , designated as (9s5p1d/4s2p1d). For H, a set of p-polarization functions,  $\alpha_p(\text{H}) = 0.75$ , was added to the Huzinaga–Dunning DZ set.

The geometries of all structures were fully optimized using the two selected DFT methods with the SDD ECP basis set. We determined the vibrational frequencies by analytically evaluating the second derivatives of the energy with respect to the nuclear coordinates at the same theoretical levels. The corresponding infrared intensities were also analytically evaluated.

All of the computations were carried out with the Gaussian 03 program.<sup>46</sup> The fine (75, 302) grid is the default for evaluating integrals numerically, and the tight ( $10^{-8}$  hartree) designation is the default for the energy convergence. The finer grid (120, 974) was used only for more carefully characterizing small imaginary vibrational frequencies.

## 3. Results

### 3.1. $\text{Cp}_2\text{M}_2(\text{CO})$ ( $\text{M} = \text{Os}, \text{Re}, \text{W}, \text{Ta}$ ) Structures.

**3.1.1.  $\text{Cp}_2\text{Os}_2(\text{CO})$ .** Four  $\text{Cp}_2\text{Os}_2(\text{CO})$  structures (Figure 3 and Table 1) in singlet, triplet, quintet, and septet spin states are predicted to be genuine minima, having all real vibrational frequencies. The singlet structure **OsI-S** is found to be the global minimum. The Os–Os quadruple bond distance of 2.31 Å is reasonable for the formal quadruple bond required to give both osmium atoms the favored 18-electron configuration for a singlet state. No experimental examples of similar compounds with Os–Os quadruple bonds are known for a direct comparison. However, the length of the original<sup>3</sup> Re–Re quadruple bond in  $\text{Re}_2\text{Cl}_8^{2-}$  is 2.24 Å.

The triplet  $\text{Cp}_2\text{Os}_2(\text{CO})$  structure **OsI-T**, lying at 6.1 (MPW1PW91) or 9.9 kcal/mol (BP86) above **OsI-S** (Figure 3 and Table 1), is predicted to have a somewhat longer Os≡Os bond length of 2.42 Å, which is consistent with the formal triple bond required for a 17-electron configuration for both osmium atoms and consistent with a binuclear triplet. The quintet and septet structures, namely, **OsI-Q** and **OsI-H**, respectively, are predicted to be very high-energy structures lying above **OsI-S** by  $35 \pm 5$  kcal/mol and  $60 \pm 8$  kcal/mol, respectively. They thus do not appear to be chemically relevant.

**3.1.2.  $\text{Cp}_2\text{Re}_2(\text{CO})$ .** Structures of  $\text{Cp}_2\text{Re}_2(\text{CO})$  with various spin multiplicities were investigated ranging from singlet to septet (Figure 4 and Table 2). The BP86 method predicts the singlet structure **ReI-S** to be the global minimum. The carbonyl bridged triplet structure **ReI-T** is predicted to lie above **ReI-S** by 8.3 kcal/mol, whereas the quintet and septet structures, namely, **ReI-Q** and **ReI-H**, lie 17.3 and 43.2 kcal/mol above **ReI-S**, respectively. However, the MPW1PW91 method predicts a triplet unbridged structure **ReI-T** to be lower in energy than **ReI-S** by 5.1 kcal/mol. The quintet and septet structures (**ReI-Q** and **ReI-H**) are predicted by MPW1PW91 to lie 2.3 and 22.9 kcal/mol, respectively, higher in energy than the singlet structure **ReI-S**. For the four predicted structures, only the quintet

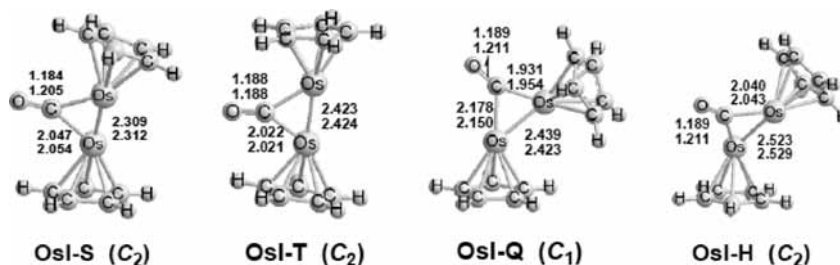


**Figure 3.** Four optimized structures of  $\text{Cp}_2\text{Os}_2(\text{CO})$ . In Figures 3 to 7, the upper bond distances (angstroms) are MPW1PW91 data and the lower bond distances are BP86 data.

**TABLE 1: Total Energies ( $E$ , in hartree), Relative Energies ( $\Delta E$ , in kilocalories per mole), Numbers of Imaginary Vibrational Frequencies (Nimag), Os–Os Bond Distances (angstroms), Infrared  $\nu(\text{CO})$  Vibrational Frequencies (inverse centimeters), and Spin Expectations  $\langle S^2 \rangle$  for  $\text{Cp}_2\text{Os}_2(\text{CO})$  Structures**

	state	OsI-S( $\text{C}_2$ ) $^1\text{A}$	OsI-T( $\text{C}_2$ ) $^3\text{B}$	OsI-Q( $\text{C}_1$ ) $^5\text{A}$	OsI-H( $\text{C}_2$ ) $^7\text{B}$
MPW1PW91	$E$	−681.83939	−681.82968	−681.79017	−681.75643
	$\Delta E$	0.0	6.1	30.9	52.1
	Nimag	0	0	0	0
	Os–Os	2.309	2.423	2.439	2.523
	$\nu(\text{CO})$	1922 (786)	1896 (722)	1886 (877)	1870 (717)
BP86	$E$	−682.16882	−682.15321	−682.10619	−682.06034
	$\Delta E$	0.0	9.9	39.3	68.1
	Nimag	0	0	0	0
	Os–Os	2.312	2.424	2.423	2.529
	$\nu(\text{CO})$	1802 (604)	1809 (634)	1756 (629)	1746 (552)
	$\langle S^2 \rangle$	0	2.01	6.02	12.02

structure **ReI-Q** is predicted to have a small imaginary vibrational frequency at  $16i \text{ cm}^{-1}$  (MPW1PW91) or  $14i \text{ cm}^{-1}$  (BP86), whereas the other three structures are predicted to be genuine minima with all real vibrational frequencies by both methods.

The 18-electron rule requires the singlet structure **ReI-S** to have a formal Re–Re quintuple bond. The Re–Re distance of

2.312 (MPW1PW91) or 2.284 Å (BP86) in the singlet structure **ReI-S** is predicted to be only slightly longer than the Re–Re quadruple bond distance<sup>3</sup> of 2.24 Å in  $\text{Re}_2\text{Cl}_8^{2-}$ . However, in terms of the metal electronic configuration in the singlet **ReI-S**, the rhenium–rhenium bond is more likely to be either a formal quintuple bond, giving both rhenium atoms the favored 18-electron configuration, or a formal triple bond, giving both

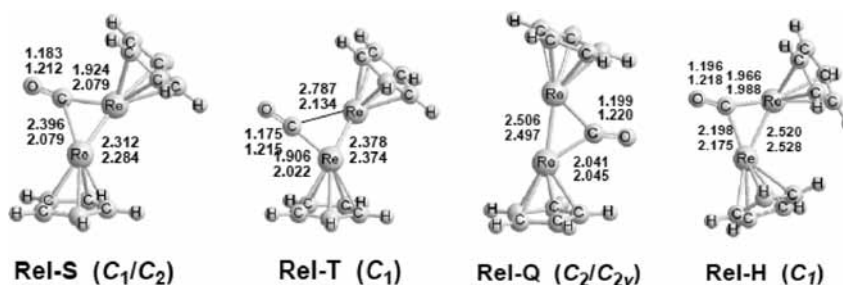


**Figure 4.** Four optimized structures of  $\text{Cp}_2\text{Re}_2(\text{CO})$ .

**TABLE 2: Total Energies ( $E$ , in hartree), Relative Energies ( $\Delta E$ , in kilocalories per mole), Numbers of Imaginary Vibrational Frequencies (Nimag), Re–Re Bond Distances (angstroms), Infrared  $\nu(\text{CO})$  Vibrational Frequencies (inverse centimeters), and Spin Expectations  $\langle S^2 \rangle$  for Structures of  $\text{Cp}_2\text{Re}_2(\text{CO})$**

	state	ReI-S( $\text{C}_1/\text{C}_2$ ) $^1\text{A}$	ReI-T( $\text{C}_1$ ) $^3\text{A}$	ReI-Q( $\text{C}_2/\text{C}_{2v}$ ) $^5\text{A}$	ReI-H( $\text{C}_1$ ) $^7\text{A}$
MPW1PW91	$E$	−656.98643	−656.99460	−656.98283	−656.94998
	$\Delta E$	0.0	−5.1	2.3	22.9
	Nimag	0	0	1(16i)	0
	Re–Re	2.312	2.378	2.506	2.520
	$\nu(\text{CO})$	1931 (933)	1980 (1136)	1829 (720)	1830 (790)
BP86	$E$	−657.31151	−657.29826	−657.28388	−657.24272
	$\Delta E$	0.0	8.3	17.3	43.2
	Nimag	0	0	1(14i)	0
	Re–Re	2.284	2.374	2.497	2.528
	$\nu(\text{CO})$	1754 (644)	1745 (608)	1725 (545)	1701 (563)
	$\langle S^2 \rangle$	0	2.01	6.03	12.03

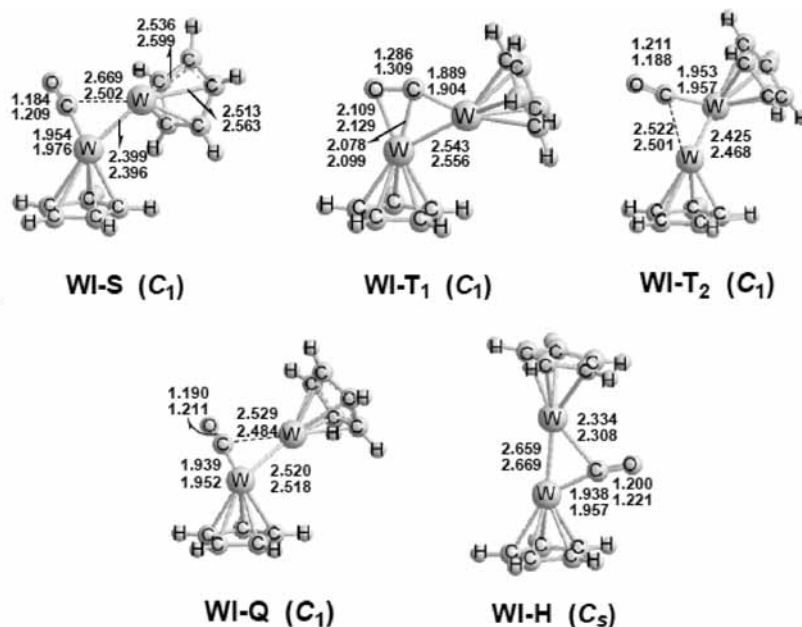


Figure 5. Five optimized structures of Cp<sub>2</sub>W<sub>2</sub>(CO).

rhodium atoms 16-electron configurations. We suspect that the sensitivity of the metal–metal bond distance to the relatively weak  $\delta$  components of quadruple and quintuple bonds is rather small. For the triplet structure **ReI-T**, the predicted Re–Re distance of 2.376 Å can be interpreted as a formal quadruple bond consistent with 17-electron configurations on both metal atoms for a binuclear triplet. For the quintet **ReI-Q** and septet **ReI-H**, the Re=Re distances of  $\sim$ 2.50 and  $\sim$ 2.52 Å are consistent with metal–metal triple bonds.

**3.1.3. Cp<sub>2</sub>W<sub>2</sub>(CO).** Five low-lying structures ranging from the singlet state to the septet state are predicted for Cp<sub>2</sub>W<sub>2</sub>(CO) (Figure 5). The global minimum of Cp<sub>2</sub>W<sub>2</sub>(CO) is an unsymmetrically bridged triplet structure **WI-T<sub>1</sub>** with all real vibrational frequencies (Table 3). The W–O distance in **WI-T<sub>1</sub>** is predicted to be very short, namely, 2.109 (MPW1PW91) or 2.129 Å (BP86), suggesting a four-electron donor bridging  $\eta^2$ - $\mu$ -CO group. This is consistent with the extremely low  $\nu$ (CO) frequency at 1445 (MPW1PW91) or 1354 cm<sup>-1</sup> (BP86) for this carbonyl group. The predicted W=W bond length in **WI-T<sub>1</sub>** of 2.543 (MPW1PW91) or 2.556 Å (BP86) can be interpreted as a formal double bond, giving both tungsten atoms 15-electron configurations for a binuclear triplet. For comparison, the experimental W=W double-bond distance in W<sub>2</sub>(OCH<sub>2</sub>tBu)<sub>8</sub>( $\mu$ -

C<sub>2</sub>H<sub>2</sub>) is found to be 2.623 Å by X-ray crystallography.<sup>47</sup> Furthermore, this tungsten–tungsten distance in **WI-T<sub>1</sub>** is rather long for the formal W–W quadruple bond required to give both tungsten atoms the usual 17-electron configurations for a binuclear triplet. Therefore, the experimentally known W–W quadruple bonds are significantly shorter, for example,  $\sim$ 2.2 Å for ditungsten tetracarboxylates,<sup>48</sup> but some of this shortening could arise from the four carboxylate bridges.

A weakly semibridged C<sub>1</sub> triplet structure **WI-T<sub>2</sub>** (Figure 5 and Table 3) was also found with all real vibrational frequencies and lying 5.3 (MPW1PW91) or 6.8 kcal/mol (BP86) above **WI-T<sub>1</sub>**. Serious spin contamination, namely,  $\langle S^2 \rangle = 2.82$ , is predicted for structure **WI-T<sub>2</sub>** by the MPW1PW91 method, which is 41% larger than the ideal value  $S(S+1) = 2$ . However, the BP86 method (which includes no exact exchange) predicts a relatively small degree of spin contamination  $\langle S^2 \rangle$  at 2.08. For the semibridging carbonyl group in **WI-T<sub>2</sub>**, the short W–C distance is  $\sim$ 1.95 Å, and the long WC distance is  $\sim$ 2.51 Å. The  $\nu$ (CO) frequency of 1880 (MPW1PW91) or 1761 cm<sup>-1</sup> (BP86) corresponds to an essentially terminal carbonyl group. The W–W distance in **WI-T<sub>2</sub>** is predicted to be 0.1 Å shorter than that in **WI-T<sub>1</sub>**, corresponding to a higher-order bond to

TABLE 3: Total Energies ( $E$ , in hartree), Relative Energies ( $\Delta E$ , in kilocalories per mole), Numbers of Imaginary Vibrational Frequencies (Nimag), W–W Bond Distances (angstroms), Infrared  $\nu$ (CO) Vibrational Frequencies (inverse centimeters), and Spin Expectations  $\langle S^2 \rangle$  for Structures of Cp<sub>2</sub>W<sub>2</sub>(CO)

	state	WI-S (C <sub>1</sub> ) <sup>1</sup> A	WI-T <sub>1</sub> (C <sub>1</sub> ) <sup>3</sup> A	WI-T <sub>2</sub> (C <sub>1</sub> ) <sup>3</sup> A	WI-Q (C <sub>1</sub> ) <sup>5</sup> A	WI-H (C <sub>s</sub> ) <sup>7</sup> A'
MPW1PW91	$E$	-634.51945	-634.56353	-634.55505	-634.55367	-634.54545
	$\Delta E$	27.7	0.0	5.3	6.2	11.3
	Nimag	0	0	0	0	1(21i)
	W–W	2.399	2.543	2.426	2.520	2.659
	$\nu$ (CO)	1916 (1106)	1445 (248)	1880 (964)	1878 (915)	1813 (665)
	$\langle S^2 \rangle$	0	2.03	2.82	6.07	12.06
BP86	$E$	-634.81610	-634.85282	-634.84189	-634.83084	-634.81522
	$\Delta E$	23.0	0.0	6.8	13.8	23.6
	Nimag	0	0	0	0	1(19i)
	W–W	2.396	2.556	2.468	2.518	2.669
	$\nu$ (CO)	1773 (795)	1354 (79)	1761 (729)	1762 (669)	1701 (483)
	$\langle S^2 \rangle$	0	2.01	2.08	6.04	12.03

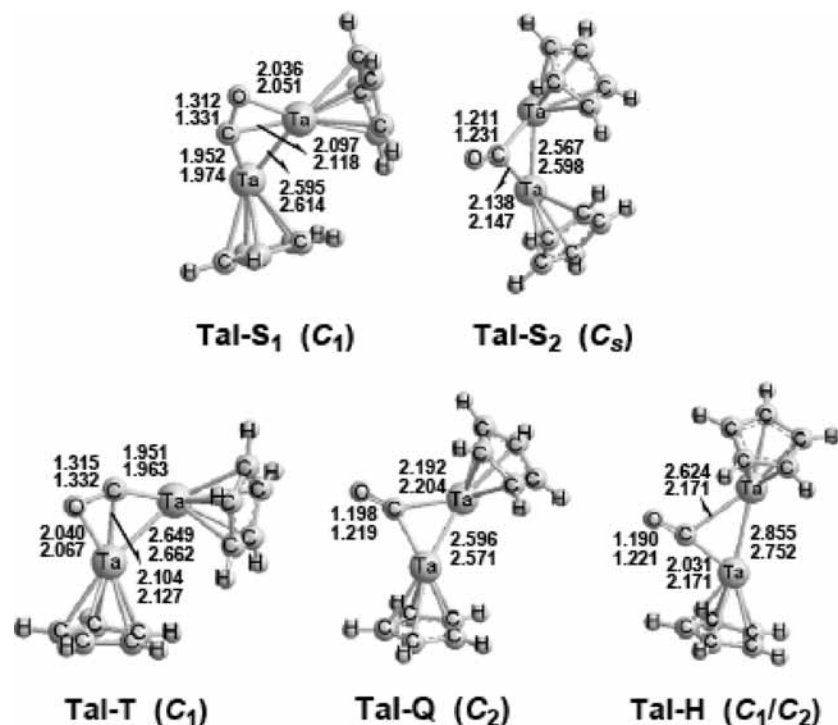


**Figure 6.** Five optimized structures of  $\text{Cp}_2\text{Ta}_2(\text{CO})$ .

compensate for the fact that the carbonyl group is a four-electron donor in **WI-T<sub>1</sub>** but only a two-electron donor in **WI-T<sub>2</sub>**.

The semibridged  $C_1$  quintet structure **WI-Q** (Figure 5 and Table 3) is predicted to lie 6.2 (MPW1PW91) or 13.8 kcal/mol (BP86) higher in energy than the global minimum **WI-T<sub>1</sub>** of  $\text{Cp}_2\text{W}_2(\text{CO})$  with all real vibrational frequencies. The W–W distance in **WI-Q** is very close to that in **WI-T<sub>1</sub>**, namely, 2.520 (MPW1PW91) or 2.518 Å (BP86), indicating a similar formal bond order. The higher spin of **WI-Q** relative to **WI-T<sub>1</sub>** compensates for the fact that the carbonyl group in **WI-Q** is a two-electron donor but that in **WI-T<sub>1</sub>** is a four-electron donor.

The septet  $\text{Cp}_2\text{W}_2(\text{CO})$  structure **WI-H** is predicted to lie 11.3 (MPW1PW91) or 23.6 kcal/mol (BP86) above **WI-T<sub>1</sub>** with a small imaginary vibrational frequency at  $21i$  MPW1PW91) or  $19i$   $\text{cm}^{-1}$  (BP86) corresponding to the rotation of one Cp ring. The W–W distance in **WI-H** is predicted to be 2.659 (MPW1PW91) or 2.669 Å (BP86), which is 0.14 Å longer than that of the quintet structure **WI-Q**.

The semibridged  $C_1$  singlet structure **WI-S** is predicted to be a genuine minimum with no imaginary vibrational frequen-

cies. However, it is a relatively high-energy structure, lying 27.7 (MPW1PW91) or 23.0 kcal/mol (BP86) above **WI-T<sub>1</sub>**. The W–W distance at 2.399 (MPW1PW91) or 2.396 Å (BP86) in **WI-S** is predicted to be the shortest of the five predicted structures of  $\text{Cp}_2\text{W}_2(\text{CO})$  and is consistent with the polarized W–W quadruple bond required to give both tungsten atoms 16-electron configurations.

**3.1.4.  $\text{Cp}_2\text{Ta}_2(\text{CO})$ .** The global minimum of  $\text{Cp}_2\text{Ta}_2(\text{CO})$  is predicted to be a bridged triplet structure **TaI-T** ( $C_1$ ), having all real vibrational frequencies (Figure 6 and Table 4). The Ta–O distance in **TaI-T** is predicted to be very short, namely, 2.040 (MPW1PW91) or 2.067 Å (BP86), suggesting a four-electron donor carbonyl. This is supported by an extremely low  $\nu(\text{CO})$  frequency of 1327 (MPW1PW91) or  $1260\text{ cm}^{-1}$  (BP86). The Ta≡Ta distance of 2.649 (MPW1PW91) or 2.662 Å (BP86) in **TaI-T** can be interpreted to be a formal triple bond giving each tantalum atom a 15-electron configuration, which is reasonable for a triplet spin state.

The singlet  $\text{Cp}_2\text{Ta}_2(\text{CO})$  structure **TaI-S<sub>1</sub>** ( $C_1$ ) is predicted to lie 12.6 (MPW1PW91) or 6.3 kcal/mol (BP86) above **TaI-T**

**TABLE 4: Relative Energies ( $\Delta E$ , in kilocalories per mole), Numbers of Imaginary Vibrational Frequencies (Nimag), Ta–Ta Bond Distances (angstroms), Infrared  $\nu(\text{CO})$  Vibrational Frequencies (inverse centimeters), and Spin Expectations  $\langle S^2 \rangle$  for Structures of  $\text{Cp}_2\text{Ta}_2(\text{CO})$**

state		TaI-S <sub>1</sub> (C <sub>1</sub> ) <sup>1</sup> A	TaI-S <sub>2</sub> (C <sub>s</sub> ) <sup>1</sup> A'	TaI-T (C <sub>1</sub> ) <sup>3</sup> A	TaI-Q (C <sub>2</sub> ) <sup>5</sup> A	TaI-H (C <sub>1</sub> /C <sub>2</sub> ) <sup>7</sup> A
MPW1PW91	<i>E</i>	−614.39809	−614.35020	−614.41811	−614.35905	−614.35825
	$\Delta E$	12.6	42.6	0.0	37.1	37.6
	Nimag	0	1(34i)	0	0	0
	Ta–Ta	2.595	2.567	2.649	2.596	2.855
	$\nu(\text{CO})$	1332 (244)	1726 (654)	1327 (280)	1762 (600)	1835 (696)
	$\langle S^2 \rangle$	0	0	2.03	6.07	12.03
BP86	<i>E</i>	−614.67381	−614.62410	−614.68385	−614.62599	−614.60949
	$\Delta E$	6.3	37.5	0.0	36.3	46.7
	Nimag	0	1(21i)	0	0	0
	Ta–Ta	2.614	2.598	2.662	2.571	2.752
	$\nu(\text{CO})$	1262 (193)	1618 (494)	1260 (232)	1655 (464)	1652 (409)
	$\langle S^2 \rangle$	0	0	2.02	6.03	12.04

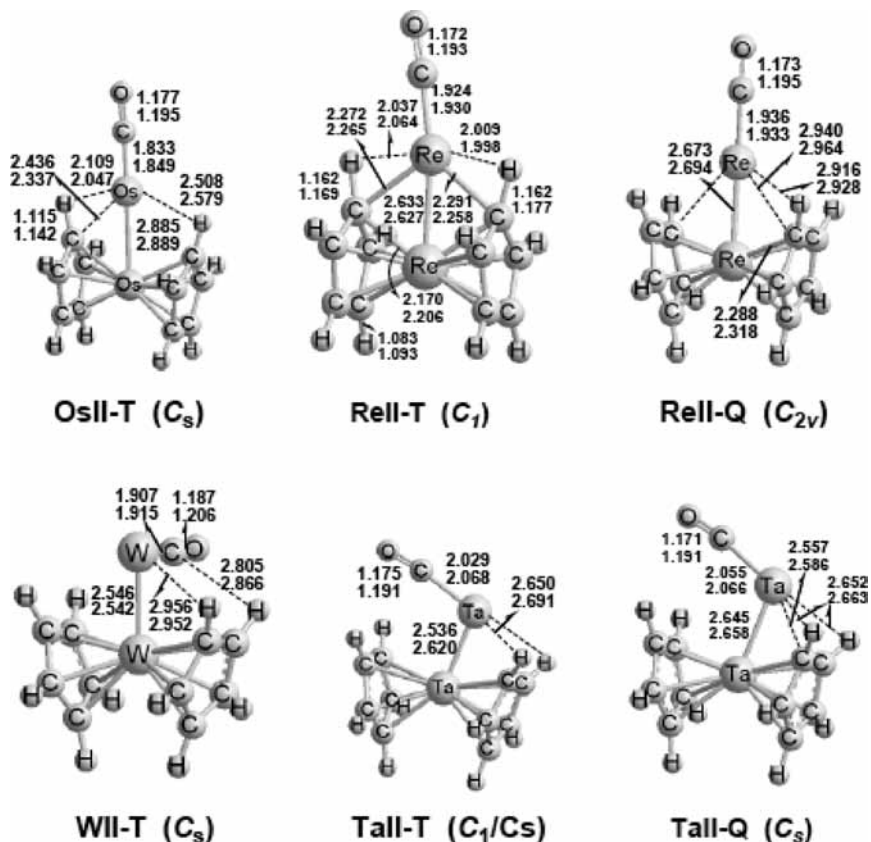


Figure 7. Optimized structures of Cp<sub>2</sub>M–M(CO) for M = Os, Re, W, Ta.

TABLE 5: Total Energies ( $E$ , in hartree), Energies ( $\Delta E$ , in kilocalories per mole) Relative to the Cp<sub>2</sub>M<sub>2</sub>(CO) Global Minimum, Numbers of Imaginary Vibrational Frequencies (Nimag), M–M Bond Distances (angstroms), Infrared  $\nu(\text{CO})$  Vibrational Frequencies (inverse centimeters), and Spin Expectations ( $S^2$ ) for Structures of Cp<sub>2</sub>M–M(CO)

	state	OsII-T ( $C_s$ ) $^3A'$	ReII-T ( $C_1$ ) $^3A$	ReII-Q ( $C_{2v}$ ) $^5B_2$	WII-T ( $C_s$ ) $^3A''$	TaII-T ( $C_1/C_s$ ) $^3A/\beta A''$	TaII-Q ( $C_s$ ) $^5A''$
MPW1PW91	$E$	−681.83806	−656.97902	−657.00153	−634.54831	−614.36580	−614.38066
	$\Delta E$	0.8	4.6	−9.5	9.5	32.8	23.5
	Nimag	0	0	0	0	0	0
	M–M	2.885	2.633	2.673	2.546	2.536	2.645
	$\nu(\text{CO})$	1997(1630)	1978(2179)	1978(1823)	1900(1132)	1920(1791)	1960(1353)
	$\langle S^2 \rangle$	2.01	2.03	6.04	2.11	2.05	6.04
BP86	$E$	−682.13538	−657.27975	−657.28597	−634.83416	−614.65099	−614.64434
	$\Delta E$	21.0	19.9	16.0	11.7	20.6	24.8
	Nimag	0	0	0	0	0	0
	M–M	2.889	2.627	2.694	2.542	2.620	2.658
	$\nu(\text{CO})$	1893(1332)	1863(1529)	1855(1416)	1805 (870)	1852(1036)	1850(1058)
	$\langle S^2 \rangle$	2.01	2.01	6.03	2.04	2.84	6.02

( $C_1$ ), having all real vibrational frequencies. A four-electron donor carbonyl group with a short Ta–O distance at 2.036 (MPW1PW91) or 2.051 Å (BP86) is predicted. An extremely low  $\nu(\text{CO})$  frequency of 1332 (MPW1PW91) or 1262 cm<sup>−1</sup> (BP86) corresponds to this four-electron donor carbonyl group. The Ta–Ta distance of **TaI-S<sub>1</sub>** is predicted to be  $\sim 0.05$  Å shorter than that in **TaI-T**.

A second much higher-energy singlet Cp<sub>2</sub>Ta<sub>2</sub>(CO) structure **TaI-S<sub>2</sub>**( $C_s$ ) with a normal bridging carbonyl is also found at  $40 \pm 3$  kcal/mol above the global minimum **TaI-T**. Structure **TaI-S<sub>2</sub>** is predicted to have an imaginary vibrational frequency at  $21i$  (MPW1PW91) or  $34i$  cm<sup>−1</sup> (BP86). Following this imaginary vibrational frequency leads to **TaI-S<sub>1</sub>**, with the normal two-electron donor bridging carbonyl in **TaI-S<sub>2</sub>** becoming a four-electron donor carbonyl group.

The quintet and septet structures **TaI-Q** and **TaI-H** of Cp<sub>2</sub>Ta<sub>2</sub>(CO) are all predicted to have a normal two-electron

donor bridging carbonyl. These structures are predicted to lie more than 35 kcal/mol above the global minimum **TaI-T** and thus are not likely to be chemically significant.

**3.2. Cp<sub>2</sub>M–M(CO) (M = Os, Re, W, Ta) Structures.** Six structures (Figure 7 and Table 5) of the type Cp<sub>2</sub>M–M(CO) (M = Os, Re, W, Ta) were investigated. These structures are of interest because both Cp rings are bonded only to one of the metals. In addition, agostic hydrogen atoms<sup>49</sup> are found in some cases. Similar Cp<sub>2</sub>M–M(CO)<sub>*n*</sub> structures have been found (but with larger numbers of carbonyl groups) in DFT studies of binuclear cyclopentadienylmetal carbonyls of molybdenum,<sup>50</sup> rhenium,<sup>51</sup> and osmium.<sup>52</sup>

The  $C_s$  triplet structure **OsII-T** (Figure 7 and Table 5) is predicted with an energy 0.8 (MPW1PW91) or 21.0 kcal/mol (BP86) above **OsI-S** (Figure 3). An agostic hydrogen atom bridging from the “left” Cp ring to the OsCO unit with an Os–H distance of 2.109 (MPW1PW91) or 2.047 Å (BP86) is predicted

**TABLE 6: Mulliken Atomic Spin Densities of CpM–M(CO) (M = Os, Re, W, Ta)**

BP86	OsII-T	ReII-T	ReII-Q	WII-T	TaII-T	TaII-Q
M <sub>1</sub> (Cp <sub>2</sub> M)	0.013	0.131	0.268	−0.134	0.748	0.852
M <sub>2</sub> (MCO)	1.953	1.832	3.590	1.972	1.174	2.484
sum of spin densities <sup>a</sup>	2.000	2.000	4.000	2.000	2.000	4.000

<sup>a</sup> This includes the spin densities on the C, H, and O atoms as well as those on the metal atom.

(Figure 7). The predicted Os–Os distance in **OsII-T**, namely, 2.885 (MPW1PW91) or 2.889 Å (BP86), can correspond to a single bond. Mulliken atomic spin densities (Table 6) of the two osmium atoms of **OsII-T** show that the two unpaired electrons are essentially localized on the OsCO osmium atom. This is consistent with the formulation of **OsII-T** as a coordination complex where an osmocene unit functions as a tridentate ligand using electron pairs from two C–H bonds as well as an osmium lone pair to bond to the OsCO group. The OsCO osmium atom is thus effectively tetracoordinate with a formal 16-electron configuration consistent with its two unpaired electrons.

A C<sub>1</sub> triplet Cp<sub>2</sub>Re–ReCO structure **ReII-T** (Figure 7) is predicted to lie above **ReI-S** (Figure 4) by 4.6 (MPW1PW91) or 19.9 kcal/mol (BP86). The Re–Re distance of **ReII-T** is predicted to be 2.633 (MPW1PW91) or 2.627 Å (BP86). Two agostic hydrogen atoms bridge from each Cp ring to the ReCO unit with predicted Re–H distances of 2.037 and 2.009 Å (MPW1PW91) or 2.064 and 1.998 Å (BP86).

The quintet Cp<sub>2</sub>Re–ReCO structure **ReII-Q** (C<sub>2v</sub>) is predicted to lie 9.5 kcal/mol lower in energy than **ReI-S** (Figure 4) by the MPW1PW91 method but 16.0 kcal/mol higher than **ReI-S** by the BP86 method. The Re=Re distance in **ReII-Q** is predicted to be 0.05 Å longer than that in **ReII-T**.

The C<sub>i</sub> triplet Cp<sub>2</sub>W–WCO structure **WII-T** (Figure 7) is predicted to lie 9.5 (MPW1PW91) or 11.7 kcal/mol (BP86) above **WI-T<sub>1</sub>** (Figure 5). The W–W distance of **WII-T** is predicted to be 2.546 (MPW1PW91) or 2.542 Å (BP86), which is consistent with a W=W double bond. The four atoms W–W–C–O are predicted to be coplanar, whereas the W–W–C angle is predicted to be very close to 90°.

The triplet and quintet structures of Cp<sub>2</sub>Ta–Ta(CO) (Figure 7), namely, **TaII-T** and **TaII-Q**, are predicted to lie >20 kcal/mol in energy above **TaI-T** (Figure 6). The Ta–Ta distances in **TaII-T** and **TaII-Q** are predicted to fall in the range of 2.536 to 2.658 Å.

#### 4. Discussion

The properties of the lowest-energy structures of the third-row transition-metal Cp<sub>2</sub>M(CO) derivatives can be compared with those of the previously studied first-row transition-metal derivatives as follows:

**4.1. Cp<sub>2</sub>Os<sub>2</sub>(CO) versus Cp<sub>2</sub>Fe<sub>2</sub>(CO).** Previous studies<sup>53</sup> on Cp<sub>2</sub>Fe<sub>2</sub>(CO) predict the lowest-energy structure by >25 kcal/mol to be a triplet structure with a bridging carbonyl group and a very short Fe<sup>δ</sup>–Fe quadruple bond distance consistent with the formal quadruple bond required to give both iron atoms the favored 18-electron configuration. Because of the triplet spin multiplicity, the quadruple bond is of the  $\sigma + 2\perp\pi + \frac{1}{2}\delta$  type, that is, with two  $\delta$  one-electron bond components rather than one two-electron  $\delta$  bond. The lowest-energy Cp<sub>2</sub>Os<sub>2</sub>(CO) structure, namely, **OsI-S**, also has a short Os<sup>δ</sup>–Os distance, indicating a formal quadruple bond. However, the singlet spin multiplicity of Cp<sub>2</sub>Os<sub>2</sub>(CO) indicates that this quadruple bond must be of the  $\sigma + 2\perp\pi + \delta$  type, that is, with a  $\delta$  two-electron bond in addition to the usual  $\sigma + 2\perp\pi$  triple bond components.

This difference is consistent with the greater tendency for spin pairing for the third-row transition metals relative to the first-row transition metals, owing to the greater ligand field splittings in third-row transition-metal complexes.

**4.2. Cp<sub>2</sub>Re<sub>2</sub>(CO) versus Cp<sub>2</sub>Mn<sub>2</sub>(CO).** The lowest-energy structure for Cp<sub>2</sub>Mn<sub>2</sub>(CO) is a septet structure with a four-electron bridging carbonyl with a quintet structure within ~1 kcal/mol of this global minimum. The septet structure for Cp<sub>2</sub>Mn<sub>2</sub>(CO) has an Mn–Mn distance consistent with the single bond required to give each manganese atom the 15-electron configuration for a binuclear septet with a four-electron bridging carbonyl. However, the lowest-energy structures for Cp<sub>2</sub>Re<sub>2</sub>(CO) are a singlet **ReI-S** by BP86 or a triplet **ReI-T** by MPW1PW91. The very short rhenium–rhenium distance in **ReI-S** is consistent with a formal quintuple bond to give each rhenium atom the favored 18-electron configuration. Again, the difference between the manganese and rhenium derivatives is an example of the tendency of the third-row transition metals to have lower spin states and higher metal–metal bond orders.

**4.3. Cp<sub>2</sub>W<sub>2</sub>(CO) versus Cp<sub>2</sub>Cr<sub>2</sub>(CO).** The lowest-energy structure predicted for Cp<sub>2</sub>Cr<sub>2</sub>(CO) is a septet with a Cr≡Cr distance indicative of the formal triple bond required to give both chromium atoms the 15-electron configuration required for a binuclear septet. For Cp<sub>2</sub>W<sub>2</sub>(CO), the lowest-energy structure is a triplet **WI-T<sub>1</sub>** with a four-electron donor bridging carbonyl group. The tungsten–tungsten bond order is not clear from the distance. However, it can be interpreted as a W=W double bond, thereby giving each tungsten atom a 15-electron configuration. This is reasonable if the tungsten atoms use only eight orbitals of their sp<sup>3</sup>d<sup>5</sup> manifolds. In any case, the triplet spin multiplicity of the lowest-energy third-row transition-metal derivative, namely, Cp<sub>2</sub>W(CO), is clearly lower than the septet spin multiplicity of the lowest-energy structure of the corresponding first-row transition-metal derivative Cp<sub>2</sub>Cr<sub>2</sub>(CO).

**4.4. Cp<sub>2</sub>Ta<sub>2</sub>(CO) versus Cp<sub>2</sub>V<sub>2</sub>(CO).** The lowest-energy structure predicted for Cp<sub>2</sub>V<sub>2</sub>(CO) is a quintet with a four-electron donor bridging carbonyl group and a V=V distance that can be interpreted as a formal double bond, thereby giving the vanadium atoms a 14-electron configuration.<sup>20</sup> For Cp<sub>2</sub>Ta<sub>2</sub>(CO), the lowest-energy structure **TaI-T** is a triplet with a four-electron donor carbonyl group and a Ta≡Ta distance suggesting a formal triple bond to give each tantalum a 15-electron configuration. This is reasonable for a binuclear triplet if one of the nine orbitals of the tantalum sp<sup>3</sup>d<sup>5</sup> manifold is not used. In summary, for all four transition-metal pairs in the Cp<sub>2</sub>M<sub>2</sub>(CO) derivatives, the lowest-energy third-row transition-metal derivative has lower spin multiplicities and higher formal metal–metal bond orders.

We also found isomeric Cp<sub>2</sub>M–MCO structures with both cyclopentadienyl rings on the same metal atom analogous to high-energy structures found in previous studies on binuclear cyclopentadienylmetal carbonyls of molybdenum, rhenium, and osmium. Using the BP86 method, we predicted the energies of all of the Cp<sub>2</sub>M–MCO structures to be at least 11 kcal/mol above the lowest-energy Cp<sub>2</sub>M<sub>2</sub>(CO) structures with one cyclopentadienyl ring on each metal atom. Mulliken spin density

analysis for the Os, Re, and W derivatives (Table 6) indicates that essentially all of the spin density is localized on the MCO metal rather than the Cp<sub>2</sub>M metal, suggesting that the Cp<sub>2</sub>M metal has the favored 18-electron configuration. For Cp<sub>2</sub>Os–OsCO (**OsII-T**), this means that the osmocene unit is acting as a donor ligand to the OsCO osmium atom, giving the latter a 16-electron configuration after considering the two agostic hydrogen atoms, leading to a predicted Os → Os distance of 2.89 Å. For Cp<sub>2</sub>Re–ReCO (**ReII-T**), this means that the Cp<sub>2</sub>Re rhenium moiety forms a formal single bond with the other rhenium atom, leading to a predicted Re–Re distance of 2.63 Å. For Cp<sub>2</sub>W–WCO (**WII-T**), this means that the tungsten in the Cp<sub>2</sub>W unit engages in a formal double bond with the other tungsten atom, leading to a predicted W=W distance of 2.54 Å. Therefore, the expected decrease in the metal–metal distances is observed in the sequence M → M, M–M, and M=M.

**Acknowledgment.** We are indebted to the 111 Project (B07012) and the National Natural Science Foundation (20873045) of China as well as the U.S. National Science Foundation (grants CHE-0749868 and CHE-0716718) for support of this research.

**Supporting Information Available:** Theoretical harmonic vibrational frequencies for Cp<sub>2</sub>M<sub>2</sub>(CO) (M = Os, Re, W, Ta) using the BP86 method, theoretical Cartesian coordinates Cp<sub>2</sub>M<sub>2</sub>(CO) (M = Os, Re, W, Ta) using the MPW1PW91 method, and complete Gaussian 03 reference (ref 46). This material is available free of charge via the Internet at <http://pubs.acs.org>.

## References and Notes

- (1) Cotton, F. A.; Walton, R. A. *Multiple Bonds Between Metal Atoms*; Wiley: New York, 1982.
- (2) Radius, U.; Breher, F. *Angew. Chem., Int. Ed.* **2006**, *45*, 3006.
- (3) Cotton, F. A.; Harris, C. B. *Inorg. Chem.* **1965**, *4*, 330–334.
- (4) Nguyen, T.; Sutton, A. D.; Brynda, M.; Fetting, J. C.; Long, G. J.; Power, P. P. *Science* **2005**, *310*, 844.
- (5) Frenking, G. *Science* **2005**, *310*, 796.
- (6) Brynda, M.; Gagliardi, L.; Widmark, P.-O.; Power, P. P.; Roos, B. O. *Angew. Chem., Int. Ed.* **2006**, *45*, 3804.
- (7) Merino, G.; Donald, K. J.; D'Acchioli, J. S.; Hoffmann, R. *J. Am. Chem. Soc.* **2007**, *129*, 15295.
- (8) Brynda, M.; Gagliardi, L.; Roos, B. D. *Chem. Phys. Lett.* **2009**, *471*, 1.
- (9) King, R. B.; Bisnette, M. B. *J. Organomet. Chem.* **1967**, *8*, 287.
- (10) Lukehart, C. M. Chapters 1 and 2. In *Fundamental Transition Metal Organometallic Chemistry*; Brooks/Cole: Monterey, CA, 1985.
- (11) Crabtree, R. H. *The Organometallic Chemistry of the Transition Metals*, 2nd ed.; Wiley: New York, 1994; pp 25–32.
- (12) Huang, J. S.; Dahl, L. F. *J. Organomet. Chem.* **1983**, *243*, 57.
- (13) Curtis, M. D.; Butler, W. M. *J. Organomet. Chem.* **1978**, *155*, 131.
- (14) King, R. B.; Efraty, A.; Douglas, W. M. *J. Organomet. Chem.* **1973**, *60*, 125.
- (15) Potenza, J.; Giordano, P.; Mastropaolo, D.; Efraty, A. *Inorg. Chem.* **1974**, *13*, 2540.

- (16) Cotton, F. A.; Kruczynski, L.; Frenz, B. A. *J. Organomet. Chem.* **1978**, *160*, 93.
- (17) Huffman, J. C.; Lewis, L. N.; Caulton, K. G. *Inorg. Chem.* **1980**, *19*, 2755.
- (18) Herrmann, W. A.; Serrano, R.; Weichmann, J. *J. Organomet. Chem.* **1983**, *246*, C57.
- (19) Hoyano, J. K.; Graham, W. A. G. *Chem. Commun.* **1982**, 27.
- (20) Li, Q.-S.; Zhang, X.; Xie, Y.; King, R. B.; Schaefer, H. F. *J. Am. Chem. Soc.* **2007**, *129*, 3433.
- (21) Ehlers, A. W.; Frenking, G. *J. Am. Chem. Soc.* **1994**, *116*, 1514.
- (22) Delly, B.; Wrinn, M.; Lüthi, H. P. *J. Chem. Phys.* **1994**, *100*, 5785.
- (23) Li, J.; Schreckenbach, G.; Ziegler, T. *J. Am. Chem. Soc.* **1995**, *117*, 486.
- (24) Jonas, V.; Thiel, W. *J. Phys. Chem.* **1995**, *102*, 8474.
- (25) Barckholtz, T. A.; Bursten, B. E. *J. Am. Chem. Soc.* **1998**, *120*, 1926.
- (26) Niu, S.; Hall, M. B. *Chem. Rev.* **2000**, *100*, 353.
- (27) Macchi, P.; Sironi, A. *Coord. Chem. Rev.* **2003**, *238*, 383.
- (28) Bühl, M.; Kabrede, H. *J. Chem. Theory Comput.* **2006**, *2*, 1282.
- (29) Tonner, R.; Heydenrych, G.; Frenking, G. *J. Am. Chem. Soc.* **2008**, *130*, 8952.
- (30) Ziegler, T.; Autschbach, J. *Chem. Rev.* **2005**, *105*, 2695.
- (31) Waller, M. P.; Bühl, M.; Geethalakshmi, K. R.; Wang, D.; Thiel, W. *Chem.—Eur. J.* **2007**, *13*, 4723.
- (32) Hayes, P. G.; Beddie, C.; Hall, M. B.; Waterman, R.; Tilley, T. D. *J. Am. Chem. Soc.* **2006**, *128*, 428.
- (33) Bühl, M.; Reimann, C.; Pantazis, D. A.; Bredow, T.; Neese, F. *J. Chem. Theory Comput.* **2008**, *4*, 1449.
- (34) Besora, M.; Carreon-Macedo, J.-L.; Cowan, J.; George, M. W.; Harvey, J. N.; Portius, P.; Ronayne, K. L.; Sun, X.-Z.; Towrie, M. *J. Am. Chem. Soc.* **2009**, *131*, 3583.
- (35) Ye, S.; Tuttle, T.; Bill, E.; Simkhovich, L.; Gross, Z.; Thiel, W.; Neese, F. *Chem.—Eur. J.* **2008**, *14*, 10839.
- (36) Becke, A. D. *Phys. Rev. A* **1988**, *38*, 3098.
- (37) Perdew, J. P. *Phys. Rev. B* **1986**, *33*, 8822.
- (38) Adamo, C.; Barone, V. *J. Chem. Phys.* **1998**, *108*, 664.
- (39) Zhao, Y.; Pu, J.; Lynch, B. J.; Truhlar, D. G. *Phys. Chem. Chem. Phys.* **2004**, *6*, 673.
- (40) Perdew, J. P. In *Electronic Structure of Solids '91 ed.* Ziesche, P., Esching, H., Eds.; Akademie Verlag: Berlin, 1991; p 11.
- (41) Zhao, S.; Wang, W.; Li, Z.; Liu, Z. P.; Fan, K.; Xie, Y.; Schaefer, H. F. *J. Chem. Phys.* **2006**, *124*, 184102.
- (42) Feng, X.; Gu, J.; Xie, Y.; King, R. B.; Schaefer, H. F. *J. Chem. Theory Comput.* **2007**, *3*, 1580.
- (43) Andrae, D.; Haussermann, U.; Dolg, M.; Stoll, H.; Preuss, H. *Theor. Chim. Acta* **1990**, *77*, 123.
- (44) Dunning, T. H. *J. Chem. Phys.* **1970**, *53*, 2823.
- (45) Huzinaga, S. *J. Chem. Phys.* **1965**, *42*, 1293.
- (46) Frisch, M. J.; et al. *Gaussian 03*, revision C 02; Gaussian, Inc.: Wallingford, CT, 2004. (See the Supporting Information for details.)
- (47) Chisholm, M. H.; Streib, W. E.; Tiedtke, D. B.; Wu, D.-D. *Chem.—Eur. J.* **1998**, *4*, 1470.
- (48) Santure, D. J.; McLaughlin, K. W.; Huffman, J. C.; Sattelberger, A. P. *Inorg. Chem.* **1983**, *22*, 1877.
- (49) Brookhart, M.; Green, M. L. H. *J. Organomet. Chem.* **1983**, *250*, 395.
- (50) Zhang, X.; Li, Q.-S.; Xie, Y.; King, R. B.; Schaefer, H. F. *Organometallics* **2009**, *28*, 2818.
- (51) Xu, B.; Li, Q.-S.; Xie, Y.; King, R. B.; Schaefer, H. F. *Inorg. Chem.* **2008**, *47*, 6779.
- (52) Xu, B.; Li, Q.-S.; Xie, Y.; King, R. B.; Schaefer, H. F. *Organometallics* **2008**, *27*, 5921.
- (53) Wang, H. Y.; Xie, Y.; King, R. B.; Schaefer, H. F. *Inorg. Chem.* **2006**, *45*, 3384.

JP903467Q